Formation of aquatic Th(IV) colloids and stabilization by interaction with Cm(III)/Eu(III)

ARTICLE *in* THE JOURNAL OF PHYSICAL CHEMISTRY B · APRIL 2006

Impact Factor: 3.3 · DOI: 10.1021/jp057091c · Source: PubMed

Formation of Aquatic Th(IV) Colloids and Stabilization by Interaction with Cm(III)/Eu(III)

Jong-Il Yun,*,† Maria-Anna Kim,‡ Petra J. Panak,† Jae-Il Kim,† and Thomas Fanghänel†,§

Institut für Nukleare Entsorgung, Forschungszentrum Karlsruhe, P.O. Box 3640, D-76021 Karlsruhe, Germany, Institut für Radiochemie, Technische Universität München, D-85748 Garching, Germany, and Physikalisch-Chemisches Institut, Ruprecht-Karls-Universität Heidelberg, Im Neuenheimer Feld 253, D-69120 Heidelberg, Germany

Received: December 6, 2005; In Final Form: February 2, 2006

The present investigation is to ascertain under what conditions actinide ions undergo aggregation via oxo-bridging to form stable colloidal species. Eu and Th are taken for this purpose as trivalent and tetravalent actinide homologue ions, respectively. For verification of the effects of impurities in chemicals on the actinide colloid generation, pH is adjusted either by a conventional acid−base titration or by coulometry without addition of NaOH. The colloid generation is monitored by highly sensitive laser-induced breakdown detection in varying pH from 3 to 7, first in dilute Eu and Th solutions separately and then in a mixture of both, all in 0.5 M HCl/NaCl. The formation of stable colloids is observed particularly in a mixed solution of Eu and Th, suggesting that aggregation via mutual oxo-bridging of trivalent and tetravalent metal ions results in surface polarization, leading to stable hydrophilic particles of 20−30 nm in diameter. When Eu is replaced by Cm in the mixed solution in favor of the high fluorescence intensity of the latter, the chemical speciation is determined on colloid-borne Cm by time-resolved laser fluorescence spectroscopy. Two different colloid-borne Cm species, oxo-bridged with Th, are identified: a minor amount at 598.0 nm (denoted as Cm−Th(1)) and a major amount at 604.8 nm (Cm−Th(2)). The former is found as a transitional state, which converts to the latter with increasing pH and prevails at pH > 5.5. Both colloid-borne species (Cm−Th) are distinctively different from hydrolyzed Cm or its carbonate complexes with respect to their fluorescence peak positions and lifetimes. In conclusion, a mixed oxo-bridging of trivalent and tetravalent actinides elicits the generation of stable colloids, whereas individual ions in their pure state form colloids under oversaturation at near neutral pH only as a transitional state for precipitation.

Introduction

The hydrolysis tendency of tetravalent actinide ions is the highest among aquatic actinide ions,[1,2] which is known to be in the following order: $An^{4+} > AnO_2^{2+} \geq An^{3+} > AnO_2^{+}$ under normal conditions. This is the reason that the solubility of tetravalent actinides is extremely low ($<10^{-9}$ M) in the near neutral pH region and beyond.[3] The same reason is attributed to polynucleation and further to colloid formation under oversaturation, as observed in many investigations.[4−11] As a result, an interface equilibration between ionic species and colloids is often regarded as being similar to the solubility equilibration.[4,5] Such colloids are called "real-colloids" of actinides, while actinides scavenged by aquatic colloids are named "pseudo-colloids" of actinides for the purpose of plain distinction between the two types.[12]

Whereas ubiquitous aquatic colloids play a significant role for the migration of actinides via forming pseudo-colloids in aquifer systems,[12−16] the migration behavior of real-colloids of tetravalent actinides remains hitherto unknown, because their stability has not been ascertained in the natural aquifer pH range. The real-colloid formation of tetravalent actinides is always observed in their solubility measurements,[4,5] when the solution is saturated in contact with precipitate. The presence of such colloids makes the apparent solubility higher, for some cases many orders of magnitude, than the true solubility. A typical example of such a phenomenon is visualized in Figure 1 for the solubility of thorium as a function of pH in an attempt to explain why the present investigation becomes necessary. The fluctuation of solubility is ascribed to the formation of colloids and their separation modus operandi, namely, ultrafiltration at different pore size, ultracentrifugation at different gravitation, precipitation at different kinetics, etc. Such a large disparity occurs only in the solubility measurement of tetravalent actinides, while the same event is not or much less observed in the solubility experiment of other oxidation states.[17,18]

The colloid formation of tetravalent actinides has been known as an obvious fact,[4,5,19] as is apparent from their charge state; consequently the highest hydrolysis tendency maintains polynucleation via oxo-bridging. The question is under what conditions colloids are formed and moreover whether they remain stable without precipitation by aging. However, ubiquitous aquatic colloids in all kinds of aqueous solutions, although they are in a trace quantity, cast doubt on their role in the formation of actinide colloids as observed, evidently more for tetravalent than other oxidation states of actinides. The present investigation is therefore to answer these questions, since they are of cardinal importance for a better understanding of the actinide migration behavior, particularly of the tetravalent oxidation state, which has been hitherto either trivialized or considered as significant. For this purpose, highly sensitive

* Author to whom correspondence should be addressed. Phone: ++49-7247-826294. Fax: ++49-7247-823927. E-mail: yun@ine.fzk.de.
† Forschungszentrum Karlsruhe.
‡ Technische Universität München.
§ Ruprecht-Karls-Universität Heidelberg.

10.1021/jp057091c CCC: $33.50
Published on Web 02/28/2006

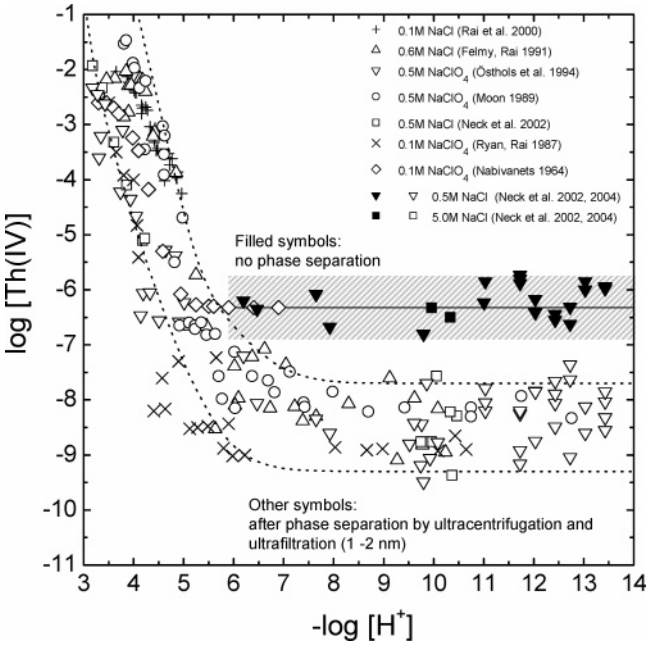

Figure 1. Solubility of amorphous thorium oxo-hydroxide and hydroxide at 0.1−5 M NaCl/$NaClO_4$ and 17−25 °C.[4−11] The dotted lines represent lower and upper limits of the solubility calculated with the solubility product of log $K^o_{sp} = -47.0 \pm 0.8$ and hydrolysis constants obtained from the literature.[3] The values reported scatter considerably with an uncertainty of several orders of magnitude, which is primarily contributed by various levels of success in removal of polymers and/or colloids. The filled symbols in the hatched region represent thorium concentrations measured without phase separation.[4,5]

experimental methods are applied, i.e., laser-induced breakdown detection (LIBD) for colloid monitoring, time-resolved laser fluorescence spectroscopy (TRLFS) for chemical speciation, and radiometric measurement for trace quantification.

Experimental Section

$Th(NO_3)_4 5H_2O$ (p.a.), Eu_2O_3 (99.99%), NaCl (p.a.), and HCl (p.a.) from Merck and NaOH of high purity (99.996%, from Alfa Aesar) are used in the present experiment. NaCl (p.a.) is recrystallized twice for purification from colloidal impurities. All solutions are prepared with Milli-Q water (academic apparatus of Millipore). Prior to each experiment, the starting solutions of europium, thorium, and a mixture of both are subjected to ultracentrifugation (Beckman XP-90) at $2 \times 10^5 g$ for 1 h to remove latent colloidal impurities. Thorium and europium concentrations are determined by inductively coupled plasma mass spectrometry (ICP-MS, Elan 6100, Perkin Elmar), before and during the experiment, in diluting to 1:10 or to 1:100 with 2% ultrapure HNO_3 (Merck).

The pH is adjusted by two different approaches. One is a common acid−base titration, and another a coulometric method without addition of alkaline solution. A combination pH electrode (ROSS type, Orion) is calibrated against standard buffer solutions (pH 1−9, Merck) for determining the H^+ concentration, which is then related to the operational pH_{exp} in 0.5 M NaCl, i.e., $-\log[H^+] = pH_{exp} + A$. The A values are determined by measuring pH_{exp} in NaCl for the acidity range of 0.001−0.1 M HCl. Further details are given elsewhere.[4,20] For the acid−base pH titration, very low metal ion concentrations are used: 6.5×10^{-7} M Th and 1.0×10^{-7} M Eu at an ionic strength of 0.03 M NaCl. Prior to the colloid generation experiment with the metal ions concerned, alone or mixed, the individual chemicals HCl and NaOH are examined for the original presence of colloidal impurities as well as for their generation upon pH change by dilution or by acid−base titration.

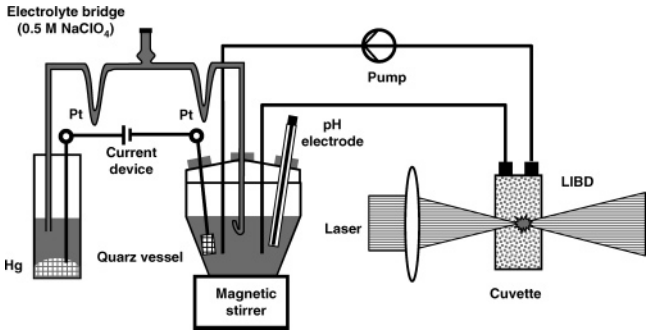

Figure 2. Experimental setup of coulometry combined to LIBD.

The coulometer is connected, as shown in Figure 2, to a LIBD apparatus to facilitate the on-line measurement of colloid generation upon pH change. A 40 mL sample in a quartz vessel of the coulometer is circulated to a flow-through optical cell of LIBD by a peristaltic pump. Two different concentration pairs are used in coulometry: first at 1.2×10^{-4} M Th and 1.8×10^{-5} M Eu and later at diluted concentrations of 1.1×10^{-6} M Th and 1.2×10^{-6} M Eu, all in 0.5 M NaCl. In the coulometric experiment, pH is controlled with a current range of 1−50 μA. In a 40 mL sample solution, applying 10 μA corresponds to adding 9 μmol [OH^-] per day. A variation of pH from 3 to 7 is executed for several weeks by changing 0.1 pH unit at each step. After pH increase, the current is turned off for 1 h to attain equilibration prior to conducting the LIBD measurement. After the LIBD measurement, the current is switched on again for further pH increase. A slightly higher current activates colloid formation due to an inhomogeneous pH change in solution, in particular, at pH close to the solubility edge of a given metal ion. This type of colloid is dissolved after attaining equilibration. At the moment of inciting colloid formation, the equilibration time is extended to ascertain whether generated colloids remain stable.

Laser-induced breakdown detection used for the colloid detection is a laser-based method, being capable of quantifying aqueous particles of smaller sizes (<100 nm) in a very dilute concentration. As the threshold irradiance necessary to generate a breakdown event is lower for solid than for liquid, the operational laser pulse energy is kept constant at a value below the threshold irradiance for the aqueous solution under investigation, e.g. ultrapure water, 0.03 M NaCl, or 0.5 M NaCl. The inception of colloid formation is recognized by a sudden increase of the breakdown probability, which is defined by the ratio of the number of breakdown events to the number of applied laser pulses. The principle and operational modus of LIBD is described elsewhere in detail.[15,21−23]

Spectroscopic speciation by TRLFS is performed to characterize the colloid-borne curium species, which are generated via interaction with thorium by increasing pH gradually from 2 to 9. Curium of isotope ^{248}Cm ($T_{1/2} = 3.6 \times 10^5$ years) is chosen, because it is a chemical homologue of Eu and optically very sensitive, owing to its fluorescence yield much superior to that of Eu.[24] Speciation is determined in a pure Cm solution (1.5×10^{-7} M) as well as in its mixture with Th (1×10^{-6} M) accompanied by an on-line pH change at about 0.5 units from pH 2 to 9 by gradual addition of diluted NaOH. Fluorescence is measured in the wavelength range between 580 and 620 nm, after excitation of Cm at its prominent absorption region at 375 nm.[25] Details of the TRLFS instrumentation are described elsewhere.[26]

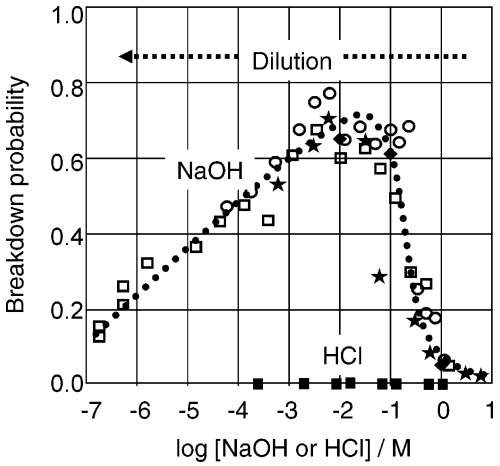

Figure 3. Colloid formation monitored by LIBD in NaOH (99.996%) upon dilution with water (18.2 MΩ cm) for a variety of starting concentrations from 1 (□, ○, ◆) to 5 mol/L (★). Dilution of 1 M HCl (■) does not show colloid formation. Decrease in the breakdown probability from 10^{-2} M NaOH is attributed to a dilution of the colloid concentration.

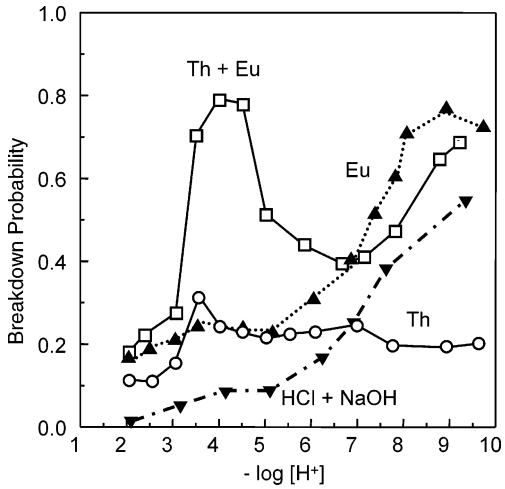

Figure 4. Colloid formation observed by LIBD as a function of pH in acid−base titration: in a blank solution, in Eu (1.0×10^{-7} M) and Th (6.5×10^{-7} M) solutions and in a mixture of both. All titrations are made with 0.03 M HCl and NaOH for increasing pH.

Results and Discussion

Colloid Formation in Acid−Base Titration. Measuring latent colloidal impurities in chemicals and the appraisal of colloid generation upon pH change by the addition of HCl and NaOH is of primary interest naturally in the beginning of the present experiment. Therefore, solutions of 1−5 M NaOH and 1 M HCl prepared freshly are diluted in succession and subjected to LIBD. The results are shown in Figure 3. The HCl solution used appears free of colloids over the range of its dilution from 1 to 10^{-4} M. In NaOH solutions (1−5 M), colloidal impurities appear to be negligible at the start, i.e., ≥1 M, but become noticeable upon dilution, increasing rapidly up to the breakdown probability of around 70% between 10^{-1} and 10^{-3} M NaOH and then decreasing gradually on further dilution to neutral pH. The decrease is found as a dilution of the once generated colloid concentration. Trace inorganic impurities are plausibly attributed to the colloid generation in NaOH (99.996% purity). Such impurities present presumably as anionic species at the high alkalinity become dissociated on dilution, exceeding their solubility with pH decrease, and undergo polynucleation via mixed oxo-bridging. The ICP-MS analysis shows the presence of inorganic impurities in NaOH, such as aluminum (7×10^{-7} M) and iron (5×10^{-6} M), and the colorimetry of β-silicomolybdic acid shows 1×10^{-5} M silicon, all of which are prone to colloid formation at near neutral pH by forming mutual oxo-bridging. The formation of colloidal metal ion−silicate, e.g. aluminosilicate, is well-known.[27,28] A notable feature is the reproducible pattern observed for the breakdown probability irrespective of the starting concentration of NaOH solutions. This means that a consistent concentration of impurities in NaOH takes part in the formation of colloids by lowering alkalinity. Extra trials with ultrafiltration or ultracentrifugation have failed to remove colloidal impurities from the original alkaline NaOH solutions.

The colloid generation is examined for the initial acidic solutions (0.03 M HCl) of Eu (1.0×10^{-7} M) and Th (6.5×10^{-7} M) as well as a mixture of both, as shown in Figure 4, by titrating with 0.03 M NaOH. In parallel, a blank titration is made with 0.03 M HCl and NaOH to examine the background effect. High-purity NaOH (99.996%, Alfa Aesar) generates colloidal impurities upon acid−base titration, same as does the pH change by dilution (cf. Figure 3). The 0.03 M HCl solution does not show the presence of colloids at the start, but with increasing pH by addition of NaOH the colloid generation progresses gradually, and the breakdown probability reaches around 50% or higher at pH ≥ 9. These values are comparable to the dilution experiment with NaOH in Figure 3 at concentration of approximately 10^{-4} M and less (equivalent to pH ≤ 10). Such a colloidal background evidently accounts for trace metal ion impurities in NaOH, which cannot be purified easily to the degree desired for the present experiment.

The acid−base titration of a dilute Eu solution shows the progressive colloid generation with increasing pH, following a similar trend as the blank acid−base titration but at a higher level. Metal ion impurities present in chemicals may have interacted with the Eu ion, and hence the colloid generation is enhanced. A dilute solution of Th shows a slight increase of the breakdown probability at a lower pH, which then remains almost constant around 22% with further increases in the pH. The pattern of colloid formation in the Th solution with increasing pH, different from that of the Eu solution, is presumably ascribed to the solubility of Th, which is much lower than that of Eu at neutral pH and beyond.[17,29] As the pH edge of the Th solubility is around 4.5, a partial precipitation of colloid-borne Th takes place slowly, and hence the precipitation and colloid generation appears counter balanced. Once the Th and Eu solutions are mixed, the pH-dependent colloid generation appears notably different from the pure solution of each element. At pH 3 the colloid generation increases drastically in the mixture, decreases at pH > 5, and follows the same trend as in the Eu solution. The presence of the Eu ion enhances the generation of thorium colloids, suggesting that mixed oxo-bridging of different oxidation states results in enhanced colloid formation. Because of colloid-forming impurities in NaOH, of which the total concentration is higher than that of Th or Eu, the precise assessment of colloid formation in metal ion and mixed solutions concerned is not possible by acid−base titration alone.

As is apparent from Figure 4, the trace metal ion impurities in chemicals have a considerable influence on appraising whether trivalent and tetravalent actinide ions form colloidal species at neutral pH and beyond. To obviate such an effect, especially that of trace impurities in NaOH, the coulometry is applied to adjust pH.

Colloid Formation in Coulometric Experiments. The pH adjustment by coulometry facilitates preserving the purity of

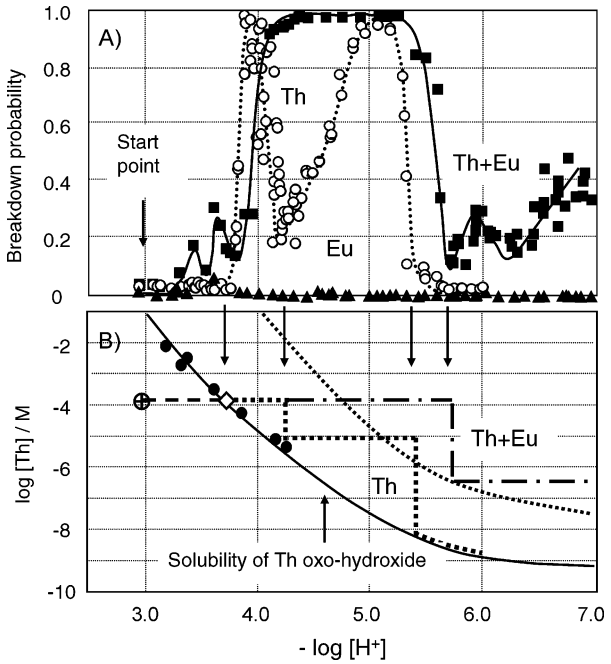

Figure 5. (A) Colloid formation as a function of pH in Eu (1.8×10^{-5} M) and Th (1.2×10^{-4} M) solutions and a mixture of both as determined by coulometric pH change in combination with LIBD. (B) The colloid generation and subsequent precipitation due to oversaturation is compared to the known solubility of Th oxo-hydroxide and hydroxide[3,4] from Figure 1. The solid line represents the lower solubility limit excluding polymers and/or colloids while the dotted line signifies the upper solubility limit including polymers and/or colloids.

experimental solutions better than acid−base titration. The results of the coulometric titration combined with LIBD are shown in the upper part of Figure 5 for the solutions of 1.8×10^{-5} M Eu, 1.2×10^{-4} M Th and a mixture of both in 0.5 M NaCl in the pH range of 3−7. The laser pulse energy is kept constant below the threshold irradiance for 0.5 M NaCl. Colloid-forming impurities in NaCl are eliminated in advance by recrystallization twice. The experimental results on all three solutions are presented together for the purpose of comparison. The lower part of Figure 5 presents the solubility of Th oxo-hydroxide (dark line) and fresh Th hydroxide (dotted line) taken from Figure 1 for convenience of interpreting the colloid generation in the Th solution as well as in the mixture solution of Th and Eu.

No colloid formation is observed in the coulometric study of the Eu solution (1.8×10^{-5} M) up to pH 7, contrary to its acid−base titration for the lower Eu concentration of 1.0×10^{-7} M (cf. Figure 4). As the Eu concentration is maintained below its solubility limit[18,29,30] in the pH range under investigation, no colloid formation is actually expected. The present results demonstrate that colloidal species of trivalent actinides may only be produced as a consequence of interaction with colloid-forming metal ion impurities present in solution, as confirmed in Figures 4 and 5.

By comparison of the upper and lower parts of Figure 5, the inception of colloid generation in the Th solution (1.2×10^{-4} M) is recognized at the pH edge of its solubility (pH 3.7), and fresh colloids prevail beyond pH 3.7 due to oversaturation. Further pH increase results in precipitation, hence leading to the next pH edge of the solubility (pH 4.2). Around this pH edge, some colloidal Th remains in the solution, about 20% of the total Th concentration. Further pH increase activates again colloid generation caused by a new oversaturation state of Th, followed subsequently by the second precipitation around pH 5.4. The remaining Th concentration beyond pH 5.4 is so low ($\ll 10^{-8}$ M Th) that the amount of colloidal Th is not precisely measurable by LIBD (probably $<10^{-9}$ M Th). In the Th solution, the colloid generation and subsequent precipitation follows the pattern of oversaturation accompanied by pH increase. Finally a typical solubility trait of Th oxo-hydroxide becomes apparent as ascertained in the lower part of Figure 5, in which the solid black circles are the LIBD experimental data determined in our laboratory[4,19] also in combination with coulometry. The solubility equilibration can be written as in

$$nTh(OH)^{3+} + (n+x)H_2O \Leftrightarrow Th_nO_{2n-x}(OH)_{2x}(ppt) + 3nH^+$$
$$\uparrow\downarrow$$
$$Th_nO_{2n-x}(OH)_y^{2x-y}(coll) + (2x-y)OH^-$$

the region of pH $\leq$ 4.2, where the Th colloidal species are in equilibrium with precipitate and their stability is pH-sensitive. When the pH is approaching near neutral, the colloidal species undergo precipitation as can be observed in Figure 5 at pH > 5.4. Therefore, the amounts of Th colloids observed at pH 4.2 and pH > 5.4 are distinctively different.

As a result, the present experiment demonstrates that the real-colloid formation of tetravalent actinides can be ruled out in the high-purity solution, when the pH is approaching neutral. Metal ion impurities present in solution may instigate the generation of stable colloid-borne species of tetravalent actinides as observed in Figure 4. To verify this hypothesis, the same Th solution mixed with Eu (1.8×10^{-5} M) is examined in a consistent procedure.

In the mixed solution of Th and Eu, the pattern of colloid generation as a function of pH is distinctively different from that in the Th solution. As can be seen in Figure 5, the colloid generation oscillates already below the pH edge of the Th solubility (pH 3.7), followed by a sharp increase beyond its pH edge (pH > 3.7). Generated colloids remain in the solution without precipitation up to pH 5.5 and above this pH undergo precipitation partially. Concentrations of Th measured by ICP-MS at pH 5.5 and 7.8 are 2.5×10^{-7} and 1.0×10^{-8} M, respectively, in the presence of 1.8×10^{-5} M Eu. These Th concentrations are much higher than the solubility of Th oxo-hydroxide at the corresponding pHs, i.e., 6.3×10^{-9} and 5.0×10^{-10} M, respectively. The data suggest that in the mixed solution the predominant Th species are colloidal, i.e., over 95%, at pH > 5.5. The generation of the stable colloid-borne Th species in the mixed solution is presumably attributed to the mixed oxo-bridge configuration of trivalent and tetravalent metal ions. As a consequence, the hydrophilic nature of thus ensuing colloids is enhanced by the surface polarization.

As the initial colloid formation depends on the metal ion concentration, the aforementioned experiment is repeated with lower concentrations, Th solution at a concentration of 1.1×10^{-6} M and its mixture with 1.2×10^{-6} M Eu, to ascertain the concentration effect. The results are shown in Figure 6. In the Th solution, no colloid generation is observed up to pH 5.0, although the solubility pH edge of Th oxo-hydroxide is expected at pH 4.5. The colloid generation can be appreciated only at pH $\geq$ 5 with large scattering, so far in a small amount, which decreases slowly with increasing pH. At the same time the Th concentration decreases in accordance with the solubility of its oxo-hydroxide. The precipitation occurs on the vessel surface as adsorption. The observed colloid formation in the Th solution, as shown in Figure 6, is attributed in reality to the flocculation of precipitate settled primarily on the vessel surface. Contrary to the Th solution, the colloid generation becomes clearly

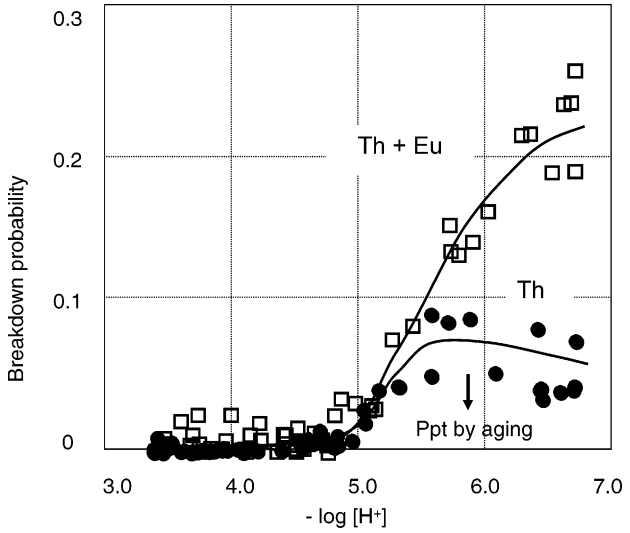

Figure 6. Colloid formation as a function of pH in the lower concentration of Th (1.1×10^{-6} M) and its mixture with Eu (1.2×10^{-6} M) as determined by coulometric pH change in combination with LIBD.

distinguishable at pH > 5 in the mixed solution of Th and Eu. The amount of colloids increases steadily with increasing pH, signifying once more that a mixture of metal ions of different oxidation states favors the colloid generation. The Th concentration in the mixed solution decreases also with pH increase but remains over 5 times higher than that in the Th solution. This tendency is similar for the experiment with the mixed solution with the higher Th concentration as shown in Figure 5.

In the two experiments given in Figures 5 and 6, the average size of stable colloids made of Th and Eu, as determined by LIBD, is found to be 20−30 nm in diameter and remains unchanged over 30 days. In the dilute Th concentration, a gradual increase of colloid size over 100 nm by aging indicates a slow conversion to precipitation, of which the rate depends on the extent of oversaturation.

Enhancement of the Th colloid generation in the presence of Eu suggests that their interaction takes place to build a mixed oxo-bridging via mutual aggregation, when the two metal ions become hydrolyzing and/or under the condition when one of the two ions is oversaturated. The process can be compared with the aggregation of metal ions in coprecipitation. Further investigation is pursued by TRLFS for the chemical speciation of colloidal species resulted from the interaction between trivalent and tetravalent metal ions.

Spectroscopic Speciation. Spectroscopic speciation is performed on the mixed solution starting at pH 2 and increasing progressively up to pH 9. For this purpose, Eu(III) is replaced by Cm(III) in favor of the better fluorescence sensitivity of the latter. This study is carried out for a mixed solution of 1.5×10^{-7} M Cm and 1×10^{-6} M Th prepared in 0.03 M HCl. The speciation is performed on-line by acid−base titration, recording a spectrum at about 0.5 pH unit intervals. To assess the impurity effect of acid−base titration, the Cm solution is examined separately in the same pH range.

The evolution of the Cm emission spectrum is shown in Figure 7 as a function of pH, for which selection of the spectrum made for a better visualization. A peak deconvolution performed to all recorded spectra from pH 2 to 9 results in three distinctive spectra as shown in the bottom of Figure 7. The spectral contribution with the two complexes together with the Cm^{3+} aquo ion is clearly observed at pH 5.6. Details on the peak deconvolution are given elsewhere.[26,28] Peak maxima of these

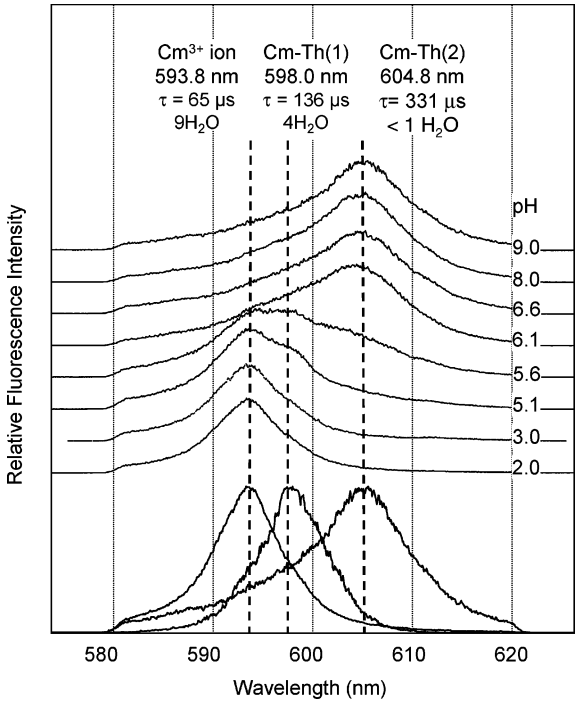

Figure 7. Speciation of colloid-borne Cm by TRLFS in a mixture of 1.5×10^{-7} M Cm and 1.0×10^{-6} M Th. Acid−base titration is applied in the pH range of 2−9. Deconvolution of composite spectra results in three different Cm species, Cm^{3+} aquo ion at 593.8 nm and two colloid-borne Cm species, Cm−Th(1) at 598.0 nm and Cm−Th(2) at 604.8 nm, which have fluorescence lifetimes of 136 and 331 μs, respectively. The observed decay rate (corresponding to the reciprocal lifetime, τ^{-1}) correlates linearly with the hydration number of curium in the first coordination sphere.[31]

spectra are located at 593.8, 598.0, and 604.8 nm, which are attributed to the Cm^{3+} aquo ion and two aggregations of Cm and Th, respectively. The latter two spectral peaks are assigned to the colloidal species of Cm−Th(1) and Cm−Th(2), respectively. The lifetime of each fluorescence peak is found to be 65 μs at 593.8 nm, 136 μs at 598.0 nm, and 331 μs at 604.8 nm. The red shift of the fluorescence band is attributed to a change in the ligand field of the Cm^{3+} aquo ion through formation of inner-sphere complexes. Since the speciation experiment is performed by acid−base titration, the effects of impurities in solution on the formation of colloidal Cm−Th(1) and Cm−Th(2) species are carefully examined in the following by comparing the spectroscopic characteristics of all components possibly involved.

A similar speciation experiment in the absence of Th is performed on the Cm solution at a concentration of 1.5×10^{-7} M. Selected results are shown in Figure 8 for increasing pH, together with the spectroscopic results for the mixed solution of Cm and Th. In the absence of Th, three different Cm species are observed: the Cm aquo ion at 593.8 nm, the first colloidal Cm(I) species at 598.0 nm, and the second colloidal Cm(II) species at 603.5 nm. The sum of Cm(I) and Cm(II) is very low, decreasing with increasing pH. The colloidal Cm(I) species appears at pH 4.0, where Cm hydrolysis is not probable at 1.5×10^{-7} M, implying that Cm is sorbed onto colloidal impurities generated during the acid−base titration. Because of the low fluorescence intensity and very broad band, the lifetime of Cm(I) species can only be estimated as less than 80 μs. The colloidal Cm(II) species has a lifetime of 83 μs, suggesting also that Cm sorbed onto colloidal impurities. The peak positions and lifetimes of Cm(I) and Cm(II) are comparable to the formation of hydrolyzed Cm species, $Cm(OH)^{2+}$ and $Cm(OH)_2^{+}$,[32]

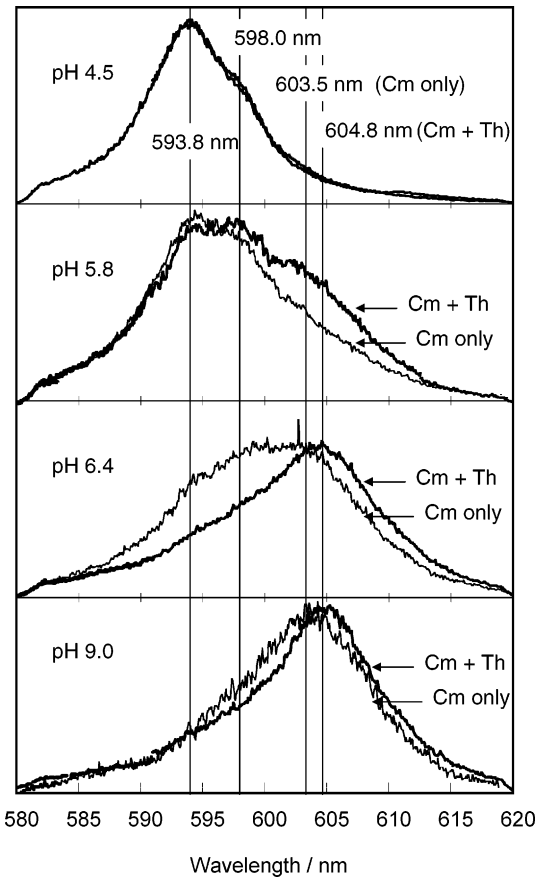

Figure 8. Comparison of Cm species monitored by TRLFS in a Cm solution (1.5×10^{-7} M) and its mixture with Th (1.0×10^{-6} M) to ascertain the effect of colloid generation in acid−base titration on the formation of the Cm−Th(1) and Cm−Th(2) species given in Figure 7. (See text for details.)

of which the emission peaks appear at 598.8 and 603.5 nm with the corresponding lifetimes of 72 and 80 μs, respectively. However, the first hydrolysis appears at pH > 6, and the second at pH > 7, whereas in the present experiment Cm(I) appears already at pH 4.0, and Cm(II) at pH 5.0, where hydrolysis of Cm at 1.5×10^{-7} M is not expected. Differences in the comparison explain that the species observed as Cm(I) and Cm(II) are ascertained as colloid-borne, i.e., Cm bound onto the surface of colloidal impurities.

Fluorescence peaks of Cm(I) and Cm(II) may overlap those of Cm−Th(1) and Cm−Th(2). Nonetheless, a comparison of each corresponding pair of lifetimes, i.e., <80 μs vs 136 μs for Cm(I) vs Cm−Th(1) and 83 vs 331 μs for Cm(II) vs Cm−Th(2), indicates that the formation of Cm(I) and Cm(II) species is largely suppressed in the presence of the Th ion. Another concern is possible contamination with CO_2 during the experiment that may lead to the carbonate complexation of the Cm^{3+} aquo ion. Carbonate complexes of Cm reveal fluorescence characteristics of 598.5, 603.0, 605.7, and 607.5 nm for $Cm(CO_3)^+$, $Cm(CO_3)_2^-$, $Cm(CO_3)_3^{3-}$, and $Cm(CO_3)_4^{5-}$, respectively.[33] Although these fluorescence peaks may overlap those of Cm−Th(1) and Cm−Th(2), the distinctive difference in each corresponding pair of lifetimes[33,34] suggests that the influence of the Cm carbonate complexation can be ruled out in the present experiment.

The relative quantification of each Cm species in the mixed solution of Cm and Th is presented in Figure 9. The first colloid-borne curium species, Cm−Th(1), appears as a minor quantity with a maximum amount of 20% around pH 5.5 and disappears

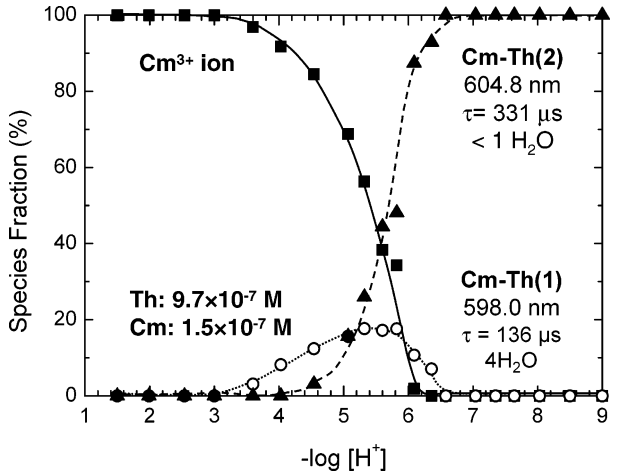

Figure 9. Distribution of different Cm species as a function of pH, as quantified by peak deconvolution of the fluorescence spectra given in Figure 7.

with further increases in pH. The second colloid-borne species, Cm−Th(2), begins to emerge at pH 4.5, grows rapidly, and prevails at pH > 6. Both LIBD and TRLFS results (Figures 6 and 9, respectively) can be correlated to comprehend how colloids of mixed metal ions are generated. The colloidal species of Cm−Th(1) may be considered as a transitional state, which is gradually converted to a more stable state of Cm−Th(2) by pH increase. The number of associated water molecules estimated from the fluorescence lifetime[31] of each species supports this assumption. The fluorescence lifetimes of 136 μs for Cm−Th(1) and 331 μs for Cm−Th(2) decipher hydration numbers of about 4 and <1, respectively. The hydration numbers implicate the higher stability of Cm−Th(2) than Cm−Th(1) and accordingly make a conclusion possible that the Cm ion is incorporated into a colloidal structure of Th in the former and sorbed on the colloid surface in the latter.

In summary, a mixed oxo-bridging of different oxidation states of actinides, as an example of trivalent and tetravalent ions shown above or of other polyvalent metal ions, favors the formation of stable aquatic actinide colloids. This finding positively explains why the formation of stable aquatic actinide colloids can be expected in natural aquifer systems, where a variety of omnipresent trace metal ions may interact with actinide ions, more favorably with tetravalent, to generate their pseudo-colloids.

Conclusions

The tetravalent actinide ions form colloids in their oversaturation state, which subsequently undergo precipitation by aging. The precipitation of colloids takes place at different rates depending on the initial concentration, pH, and temperature. In a pure solution free from impurities, tetravalent actinide ions do not form stable colloids in the near neutral pH region. Ubiquitous trace impurities in chemicals are found to be fostering components for the actinide colloid generation. As a result, tetravalent actinide ions with an excessive hydrolysis tendency that enhances oxo-bridging are prone to interact with metal ion impurities to become colloid-borne. The emerging effect is often perceived incorrectly as the formation of their real-colloids. Acid−base titration to adjust pH, which is a common practice for the solubility measurement, inevitably introduces trace impurities, particularly by alkaline medium, i.e., NaOH, which is for obvious reasons difficult to produce at the desired high purity. The large fluctuation of solubility, as shown

in Figure 1, is attributed apparently to the colloid formation instigated by impurities in solution.

As confirmed by this experiment, tetravalent actinides form stable colloids upon interaction with trace metal ions of other oxidation states present. Combined oxo-bridging of metal ions of different oxidation states, which are likely to hydrolyze, gives rise to the formation of stable colloids, as ascertained in the mixed solution of Th and Eu by LIBD combined with coulometry and in the mixed solution of Th and Cm by TRLFS. The present investigation provides significant insight into the formation of aquatic actinide colloids in both laboratory and natural aquifer systems. Therefore, the colloid-facilitated migration of actinides is subject to cautious investigation in detail.

References and Notes

(1) Choppin, G. R. *Radiochim. Acta* **1983**, *32*, 43.
(2) Rizkalla, E. N.; Choppin, G. R. Lanthanides and actinides hydration and hydrolysis. In *Handbook on the Physics and Chemistry of Rare Earths*; Gschneidner, K. A., Jr., Eyring, L., Choppin, G. R., Lander, G. H., Eds.; North-Holland: Amsterdam, 1994; p 559.
(3) Neck, V.; Kim, J. I. *Radiochim. Acta* **2001**, *89*, 1.
(4) Neck, V.; Müller, R.; Bouby, M.; Altmaier, M.; Rothe, J.; Denecke, M. A.; Kim, J. I. *Radiochim. Acta* **2002**, *90*, 485.
(5) Altmaier, M.; Neck, V.; Fanghänel, Th. *Radiochim. Acta* **2004**, *92*, 537.
(6) Ryan, J. L.; Rai, D. *Inorg. Chem.* **1987**, *26*, 4140.
(7) Felmy, A. R.; Rai, D.; Mason, M. J. *Radiochim. Acta* **1991**, *55*, 177.
(8) Östbols, E.; Bruno, J.; Grenthe, I. *Geochim. Cosmochim. Acta* **1994**, *58*, 613.
(9) Rai, D.; Moore, D. A.; Oakes, C. S.; Yui, M. *Radiochim. Acta* **2000,** *88* (5), 297.
(10) Moon, H. C. *Bull. Korean Chem. Soc.* **1989**, *10*, 270.
(11) Nabivanets, B. I.; Kudritskaya, L. N. *Ukr. Khim. Zh.* **1964**, *30*, 891.
(12) Kim, J. I. *Radiochim. Acta* **1991**, *52*, 71.
(13) McCarthy, J. F.; Zachara, J. M. *Environ. Sci. Technol.* **1998**, *23* (5), 496.
(14) Kersting, A. B.; Dfurd, D. W.; Finnegan, D. L.; Rokop, D. J.; Smith, D. K.; Thompson, J. L. *Nature* **1999**, *397*, 56.
(15) Hauser, W.; Geckeis, H.; Kim, J. I.; Fierz, T. *Colloids Surf., A* **2002**, *203* (1−3), 37.
(16) Ryan, J. N.; Elimelech, M. *Colloids Surf., A* **1996**, *197*, 1.
(17) Stadler, S.; Kim, J. I. *Radiochim. Acta* **1998**, *44*, 39.
(18) Neck, V.; Fanghänel, Th.; Kim, J. I. *Report FZKA 6110*; Forschungszentrum Karlsruhe: Karlsruhe, Germany, 1998.
(19) Bitea, C.; Müller, R.; Neck, V.; Walther, C.; Kim, J. I. *Colloids Surf., A* **2003**, *217*, 63.
(20) Altmaier, M.; Metz, V.; Neck, V.; Müller, R.; Fanghänel, T. *Geochim. Cosmochim. Acta* **2003**, *67* (19), 3595.
(21) Scherbaum, F. J.; Knopp, R.; Kim, J. I. *Appl. Phys. B* **1996**, *63*, 299.
(22) Bundschuh, T.; Knopp, R.; Kim, J. I. *Colloids Surf., A* **2001**, *177*, 47.
(23) Walther, C. *Colloids Surf., A* **2003**, *217*, 81.
(24) Kim, J. I.; Klenze, R.; Wimmer, H. *Eur. J. Solid State Inorg. Chem.* **1991**, *28*, 347.
(25) Klenze, R.; Kim, J. I.; Wimmer, H. *Radiochim. Acta* **1991**, *52*/*53*, 97.
(26) Chung, K. H.; Klenze, R.; Park, K. K.; Paviet-Hartmann, P.; Kim, J. I. *Radiochim. Acta* **1998**, *82*, 215.
(27) Kim, M. A.; Panak, P. J.; Yun, J.-I.; Kim, J. I.; Klenze, R.; Köhler, K. *Colloids Surf., A* **2003**, *216*, 97.
(28) Panak, P. J.; Kim, M. A.; Yun, J.-I.; Kim, J. I. *Colloids Surf., A* **2003**, *227*, 93.
(29) Baes, C. F.; Mesmer, R. E. *The Hydrolysis of Cations*; Wiley: New York, 1976.
(30) Yun, J.-I.; Bundschuh, T.; Neck, V.; Kim, J. I. *Appl. Spectrosc.* **2001**, *55* (3), 273.
(31) Kimura, T.; Choppin, G. R. *J. Alloys Compd.* **1994**, *213*, 313.
(32) Wimmer, H.; Klenze, R.; Kim, J. I. *Radiochim. Acta* **1992**, *56* (2), 79.
(33) Fanghänel, Th.; Weger, H. T.; Könnecke, Th.; Neck, V.; Paviet-Hartmann, P.; Steinle, E.; Kim, J. I. *Radiochim. Acta* **1998**, *82*, 47.
(34) Kim, J. I.; Klenze, R.; Wimmer, H.; Runde, W.; Hauser, W. *J. Alloys Compd.* **1994**, *213*, 333.